Oxygen Isotope Systematics and Al-Mg Chronology of Chondrules: Implications to Protoplanetary Disk Evolution.

N. T. Kita[1], [1]WiscSIMS, Department of Geoscience, University of Wisconsin-Madison, WI 53706, USA.

Introduction: Chondrules in each group of chondrite show characteristic sizes, chemical compositions, and oxygen isotope ratios, indicating that each chondrite group sampled materials in a specific region of the protoplanetary disk [1]. By using secondary ion mass spectrometer (SIMS) at the University of Wisconsin-Madison (WiscSIMS), we have been conducting high precision oxygen isotope analyses of 30-40 chondrules in multiple chondrite groups (LL3, H3, Acfer 094, CO3, CV3, CH3, CR3, R3, and Y-82094 [2-10]). The Al-Mg chronology of some of these chondrules (in LL3, Acfer 094, CO3, and CR3) further constrains the temporal evolution of the isotope reservoirs [11-15]. These analyses were performed mostly from chondrules in types 3.0-3.2 chondrites that best preserved primary isotope characters of chondrules. Here, the major findings from our recent chondrule studies are summarized and the implications to protoplanetary disk evolution are discussed.

Internal oxygen isotope homogeneity: Earlier studies indicated that oxygen isotope ratios of chondrules are internally heterogeneous as a result of incomplete isotope exchange between ^{16}O-rich solid (or melt) and ^{16}O-poor nebula gas [16-17]. However, high precision SIMS oxygen isotope analyses of minerals and glass from individual chondrules in Acfer 094 (ungrouped C3.00) show homogeneous oxygen isotope ratios, excluding relict olivine grains [4]. These results suggest that chondrule melt was homogeneous in oxygen isotope rations, which did not change during the crystallization. Similarly, oxygen isotope ratios of olivine, pyroxene, and plagioclase are indistinguishable in the individual chondrules from CR3 [6] and Y-82094 (ungrouped C3.2 [10]). Other chondrite data [2-3,5,7,9] also show agreements between oxygen isotope ratios of olivine and pyroxene within a chondrule, excluding relict olivine, in contrast to earlier study by [17].

Chondrule formation would have occurred in the dust-enriched disk at least ×100 compared to solar nebula conditions [18]. If oxides in chondrule melt were in open system during the high temperature heating [19], the oxygen isotope ratios in ambient gas would be very similar to those of average solid precursors in the local disk and might easily homogenized with chondrule melt [2, 4].

PCM line: The SIMS olivine and pyroxene analyses of Acfer 094 chondrules [4] plot between CCAM (Carbonaceous Chondrite Anhydrous Mineral [20]) and Y&R (Young and Russell [21]) lines, which are reference slope ~1 lines defined from minerals in Ca, Al-rich inclusions (CAIs). The regression of Acfer 094 data defines a new slope ~1.0 line (Fig. 1),

which passes through data from terrestrial mantle, primitive achondrites, CAIs and cosmic symplectite (COS [22]). Chondrules in all other C chondrites, as well as unusual ^{16}O-rich chondrule data from LL3 and EH [2, 23], plot on the PCM line. Therefore, the PCM line may represent primary mass independent fractionation of oxygen isotopes in the protoplanetary disk.
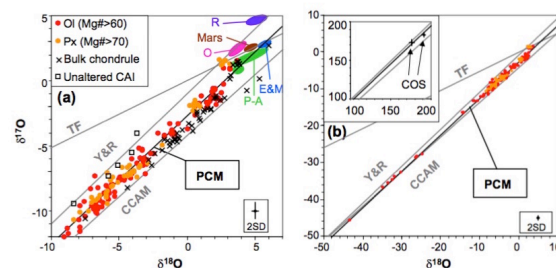
Fig. 1. Primitive chondrule mineral (PCM) line [4]. Terrestrial fractionation line (TF), CCAM, and Y&R lines are shown as references.

Mass dependent fractionation in O and R: Most chondrules in LL3, H3, and R3 chondrites plot above the TF and PCM lines [2, 7, 9]. There are large mass dependent fractionation effects between Type IA (FeO-poor and olivine-rich) to type IB (FeO-poor and pyroxene-rich) chondrules, as shown in Fig. 2. Kita et al. [2] discussed multiple processes that might fractionate oxygen isotope ratios in silicates, such as equilibrium isotope fractionation between olivine and H_2O and CO gas at high temperatures and kinetic isotope fractionation during evaporation and recondensation of oxide in chondrule melt [19].
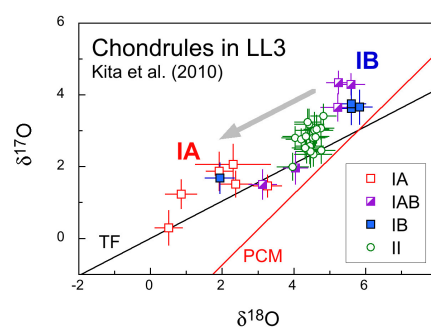
Fig. 2. Oxygen isotope ratios of chondrules in LL3 chondrites [2]. A few other data plot below TF lines are not shown. Type II (FeO-rich) chondrules show a narrow compositions.

Mg#-$\Delta^{17}O$ relationship: The FeO contents of olivine and pyroxene in chondrules, expressed as Mg# (molar [MgO] / [FeO+MgO] %), may represent oxygen fugacity during chondrule formation [6]. Oxygen isotope ratios of individual chondrules, defined by $\Delta^{17}O = \delta^{17}O - 0.52 \times \delta^{18}O$, show systematic

variations against Mg# in each chondrite group (Fig. 3). In most cases, $\Delta^{17}O$ values show discrete distributions (Fig. 3a). The $\Delta^{17}O$ values in LL3 are mostly in a narrow range of 0.5±0.9‰ (2SD) independent of Mg#. Data from H3 and R3 are very similar to those of LL3. The $\Delta^{17}O$ in CO3 and Acfer 094 show bimodal distributions; majority of chondrules with high Mg#>98 have low $\Delta^{17}O \sim -5‰$ and others have $\Delta^{17}O \sim -2$ ‰ for a wide range of Mg#. Chondrules in CV3 and Y-82094 are dominated by high Mg# chondrules with $\Delta^{17}O$ of $\sim -5‰$ [3, 10]. Cryptocrystalline chondrules in CH3 are dominated by those with $\Delta^{17}O$ values of $-2‰$ and high Mg# (>90), while minor type II chondrules have $\Delta^{17}O$ values of 1.5±0.5‰ (2SD) [8].

The $\Delta^{17}O$ values of chondrules in CR3s distribute more broadly from $-5‰$ to 0‰, showing a monotonic increase with decreasing Mg# (Fig. 3b). This trend may suggest mixing between ^{16}O-rich anhydrous dusts and ^{16}O-poor oxidizing agent, most likely water ice [24]. A simple mass balance model (Fig. 3b) indicates that type I chondrules in CR3 would have formed under the dust-enrichment of ×100-200 with variable amounts of ice [6].

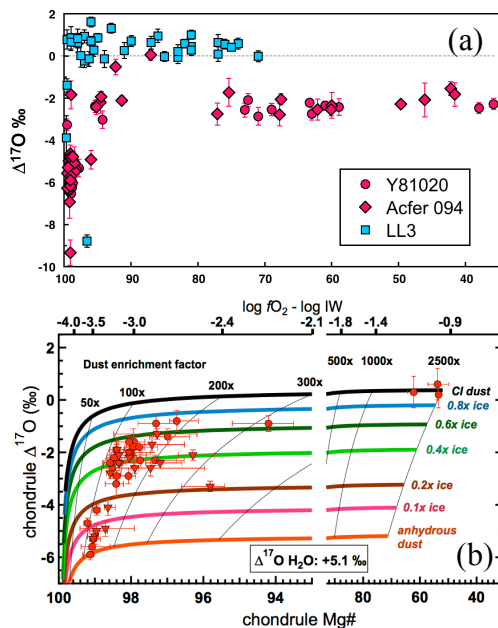

Fig. 3. Mg#- $\Delta^{17}O$ relationships among chondrules (a) CO3, Acfer 094 and LL3 [2, 4-5]. (b) CR3 data with oxygen isotope mixing model [6].

Although Mg#- $\Delta^{17}O$ relationships in other C chondrites differ from those of CR, there are significant overlaps among them. Thus, the model would be useful in understanding the environments of other chondrite groups. Chondrules with $\Delta^{17}O$ of $-5‰$ may represent those formed in dry and moderate dust-enriched conditions, which would be common in the asteroid forming regions inside the snow-line. Indeed, they are most abundant types of chondrules in CO and CV chondrites. Other chondrules with elevated $\Delta^{17}O$ values, especially abundant in CH and

CR, might have formed outside the snow line, which location could also move with disk evolution.

The model may not be applicable to chondrules in OC and RC (and also E), which might derive from the inner disk, but have higher $\Delta^{17}O$ values. Alternatively, migration of ^{16}O-poor ice to inner disk regions would result in isotope exchange between sublimated H_2O gas and ^{16}O-rich silicate dusts and produce chondrule precursor dusts with $\Delta^{17}O \sim 0$ ‰.

Early and late chondrule formation: The inferred $(^{26}Al/^{27}Al)$ ratios of chondrules in LL3, CO, and Acfer 094 all show limited ranges $(5-10)\times10^{-6}$ and do not correlate with their oxygen isotope ratios [15]. Thus, a variety of oxygen isotope reservoirs might have existed in the disk at ~2 Ma after CAI formation. In CR chondrites, many chondrules do not show resolvable excess ^{26}Mg [14, 25]. The upper limits of $(^{26}Al/^{27}Al)$ ratios are $(2-3)\times10^{-6}$, corresponding to 3 Ma after CAIs. Tenner et al. [14] found that older chondrules have $\Delta^{17}O$ values of $-5‰$, while those with $-2‰$ are younger. Late chondrule formation in CR might have occurred outside of snow line. Chondrule-like objects in Wild 2 comet show similarity to chondrules in CR for both oxygen isotope systematics and Al-Mg chronology [26-27]. Late chondrule formation processes could be related to activity of outer disk, such as the formation of Jupiter [26].

References: [1] Jones R. H. (2012) *Meteorit. Planet. Sci., 47,*1176-1190. [2] Kita N. T. et al. (2010) *GCA, 74,* 6610-6635. [3] Rudraswami N. G. et al. (2011) *GCA, 75,* 7596-7611. [4] Ushikubo T. et al. (2012) *GCA, 90,* 242-264. [5] Tenner T. J. et al. (2013) *GCA, 102,* 226-245. [6] Tenner T. J. et al. (2015) *GCA, 148,* 228-250. [7] Kita N. T. et al. (2008) *LPS 39,* #2059. [8] Nakashima D. et al. (2010) *Meteorit. Planet. Sci. Suppl., 47,* A148. [9] Kita N. T. et al. (2015) *LPS 46,* # 2053. [10] Tenner T. J. et al. (2015) *LPS 46,* #2162. [11] Kita N. T. et al. (2000) *GCA, 64,* 3913-3922. [12] Kurahashi E. et al. (2008) *GCA, 72,* 3865-3882. [13] Ushikubo T. et al. (2013) *GCA, 109,* 280-295. [14] Tenner T. J. et al. (2015) *Meteorit. Planet. Sci., Suppl. 50,* #5325. [15] Kita N. T. and Ushikubo T. (2012) *Meteorit. Planet. Sci., 47,* 1108-1119. [16] Clayton R. N. (1993) *Annu. Rev. Earth Planet. Sci., 21,* 115-149. [17] Chaussidon M. et al. (2008) *GCA 72,* 1924-1938. [18] Ebel D. and Grossman L. (2000) *GCA, 64,* 339–366. [19] Nagahara H. et al. (2008) *GCA, 72,* 1442-1465. [20] Clayton R. N. et al. (1977) *EPSL, 34,* 209-224. [21] Young E. D. and Russell S. S. (1998) *Science, 282,* 452-455. [22] Sakamoto N. et al. (2007) *Science, 317,* 231-233. [23] Weisberg M. K. et al. (2011) *GCA, 75,* 6556-6569. [24] Connolly H. C. and Huss G. R. (2010) *GCA, 74,* 2473-2483. [25] Nagashima K. et al. (2014) *Geochem. J., 48,* 561-570. [26] Ogliore R. C. et al. (2012) *ApJ., 745,* L19. [27] Nakashima D. et al. (2015) *EPSL, 410,* 54-61.